



Published in final edited form as:

*Small*. 2008 September ; 4(9): 1468–1475. doi:10.1002/smll.65476.

## An AFM/Rotaxane Molecular Reading Head for Sequence-Dependent DNA Structure\*\*

**Brian A. Ashcroft**<sup>1</sup>,

*Biodesign Institute, Arizona State University, PO Box 875601, Tempe, AZ 85287, (USA)*

**Quinn Spadola**<sup>1</sup>,

*Biodesign Institute, Arizona State University, PO Box 875601, Tempe, AZ 85287, (USA)*

**Shahid Qamar,**

*Biodesign Institute, Arizona State University, PO Box 875601, Tempe, AZ 85287, (USA)*

**Peiming Zhang,**

*Biodesign Institute, Arizona State University, PO Box 875601, Tempe, AZ 85287, (USA)*

**Gerald Kada,**

*Agilent Technologies, Nanotechnology Measurements Division Roemerstr. 18, 4020 Linz (Austria)*

**Rouvain Bension,** and

*Neotech Development Co. LLC, 310 Summit Ave., Brighton, MA 02135-7504 (USA)*

**Stuart Lindsay**

*The Biodesign Institute, Department of Physics, Department of Chemistry and Biochemistry, Arizona State University, PO Box 875601, Tempe, AZ 85281 (USA), Fax: 480-727-2378 E-mail: Stuart.Lindsay@asu.edu*

### Abstract

A nanomechanical molecular “tape reader” is assembled and tested by threading a  $\beta$ -cyclodextrin ring onto a DNA oligomer and pulling it along with an AFM tip. The formation and mechanical operation of the system is confirmed by measuring the forces required to unfold secondary structures in the form of hairpins. Unfolding induced by this 0.7 nm aperture requires 40 times more force than that reported for pulling on the ends of the DNA. A kinetic analysis shows that much less strain is required to destabilize the double helix in this geometry. Consequently, much more force is required to provide the free energy needed for opening. DNA secondary structure may prove to be a significant obstacle both for enzymes that process DNA through an orifice, and for the passage through nanopores proposed for some novel sequencing schemes.

### Keywords

AFM; Biophysics; DNA Structure; Force microscopy

---

\*\*This work was supported by the DNA sequencing technology program of the NHGRI and by DARPA. We thank Jan Liphardt for useful discussions.

Correspondence to: Stuart Lindsay.

<sup>1</sup>These authors contributed equally to this work.

## 1. Introduction

In nature, enzymes encircle biopolymers, forming rotaxanes to avoid falling off as they read, exemplified by the sliding clamp subunit of DNA polymerase.[1] Here we report an AFM-based molecular reading device for determining the force required for sequence related features of nucleic acids to pass through a small encircling orifice. The system is sensitive enough to measure unfolding of nucleic acid secondary structures. Most current single-molecule measurement techniques pull biomolecules apart by applying stress to each end of the polymer chain, a stretching process that might result in an unfolding pathway different from the shear force imposed by a sliding clamp.[2,3] Optical tweezers have been used to measure the electrophoretic force on a single DNA molecule translocating through a nanopore.[4] Protein pores have been used to trap DNA molecules[5] and the force required to open hairpins has been inferred from studies of electrophoretically-driven transit through these pores.[6–8] There do not appear to be any direct measurements of the force required to unfold secondary structure sequentially by pulling a polymer through an orifice (or, as is the case here, the orifice over the polymer). The present construct may prove expandable to a variety of studies that require sequential processing, serving as a model system for an enzyme processing a nucleic acid, and potentially providing a method for sequencing heteropolymers like DNA and proteins at the monomer level.[9]

A molecular reading head that resembles the sliding clamp of DNA polymerase was self-assembled on a threading molecule, forming a rotaxane[10,11] by locking each end of the thread with a large stopper[12] In contrast to conventional rotaxanes, one stopper is the surface to which the DNA is to be tethered, covered with anchors for the threading molecule scattered in a non-stick layer (Figure 1A). The assembly sequence is as follows:

Adamantanedicarboxylic acid is attached to the anchor, diaminododecane to the adamantane, and the resulting threading molecule (with a free amino end) spontaneously complexes functionalized  $\beta$ -cyclodextrin ( $\beta$ -CD), the smallest CD that fits over ssDNA. A poly(ethylene glycol) molecule (PEG) is attached to the free end of the dodecyl group to function as a temporary stopper. It holds the  $\beta$ -CD in place until it is pulled onto the PEG by an AFM. Finally, a DNA molecule is attached to the free end of the PEG. Translocation of the  $\beta$ -CD, and simultaneous force read-out, is achieved by fishing with a PEG “line” for a thiol group on the  $\beta$ -CD, the fishing “rod” being an atomic force microscope (AFM) probe. When the two PEG molecules are fully extended into a linear structure, the (shorter) DNA is lifted entirely from the surface, so that force signals beyond this point must result from interactions with the DNA and not with the surface. The steps required to accomplish this assembly of the CD/DNA rotaxane are shown in Figure 2. Full details of the synthesis and characterization of this system are given in the experimental section and the Supporting Information online.

## 2. Results

### 2.1 CD/DNA rotaxanes without secondary structure

Silicon AFM probes bearing vinylsulfone functionalized PEG (MW: 3200 Dalton ) were used to capture freshly deprotected thiolated  $\beta$ -CDs. Force curves were obtained in 50 mM phosphate buffer solution (PBS, pH = 7). using the liquid cell of a Picoplus AFM (Molecular Imaging/Agilent).

The formation of surface-tethered rotaxanes was verified using a test sample consisting of a 5'-thiolated oligo-T stoppered at its 3' end with a Texas Red dye molecule (Figure 3A). Fully extended, this molecule has a length of 21.4 nm (using a stretched base-to-base distance of 0.61 nm [13]). Each PEG linker (one on the surface and one on the probe – see Figure 1) has a Gaussian distribution of fully-stretched lengths with a mean value of 28 nm and a half-width at half-height (HWHH) of 2.8 nm (arising mainly from polydispersity but also including

geometric uncertainties in the position of the apex of the probe with respect to the attachment point of the polymer on the surface [14]). The other minor linking components add a further 4.4 nm at the surface and 1.2 nm at the probe (Supporting Information). In consequence, the cyclodextrin-DNA interaction cannot occur until the probe and surface are separated by  $62 \pm 5.6$  nm.

Examples of force curves showing features beyond 62 nm are given in Figure 3B. These curves are reasonably [15] well fitted by the worm-like chain (WLC) model of polymer stretching [16] with peak lengths ( $L_C$ ) near the  $21 + 62 = 83$  nm expected. The peak forces ( $f_p$ ) were  $\approx 1$  nN. Such large forces are characteristic of the breaking of covalent bonds [17] an event expected when the AFM tip keeps pulling even after the CD has reached the Texas Red stopper group. Control experiments using DNA that lacked a large stopper did not show these large force peaks (Supplementary Materials). The distribution of measured peak forces is shown in Figure 3D. The largest peak forces in control experiments (white bars) lacking a  $\beta$ -CD, or using an unfunctionalized  $\beta$ -CD, were significantly smaller than the largest peak forces measured for the full construct (black bars).

The distribution of fitted contour lengths is shown in Figure 3C (black bars). There are many events below 62 nm, but these are also observed in control experiments (white bars) in which the  $\beta$ -CD was not functionalized or was omitted entirely. Thus, the features below 62 nm correspond to various types of non-specific interaction between the components of the system. The mean length of all pulls with features above 62 nm lies near the predicted mean of 82 nm and the distribution follows a Gaussian with a HWHH close to the expected 5.6 nm. Persistence lengths determined from the WLC fits were spread over a range of values (Table I) in the vicinity of the 0.2 to 0.4 nm expected for this combination of polymers (Supporting Information). This good agreement between the predicted maximum pulling length (and its distribution), persistence length and bond breaking forces (for *all* curves showing features at distances  $>62$  nm) is strong evidence of the successful preparation of the construct shown in Figure 1.

## 2.2 CD rotaxanes passing DNA containing hairpins

In order to examine the interaction of the  $\beta$ -CD with DNA forming secondary structure, we used 49-base and an 81-base oligonucleotides, each forming two hairpins. A double-hairpin construct addresses the question of whether or not it is the hairpin structure yielding to give the force peak, because a second peak could not occur if the first were a consequence of some other bond-breaking process in the system. This is exactly analogous to the use of poly-proteins in the force spectroscopy of protein unfolding processes. [18] The lowest energy structures predicted for these oligomers by mFold ([www.bioinfo.rpi.edu/applications/mfold/](http://www.bioinfo.rpi.edu/applications/mfold/)) are shown in Figures 4A and B.

The force curves (Figures 4C and D) are strikingly consistent with the passage of two hairpins, many showing two surprisingly large features. The force maxima for the 81-base oligomer clearly occur at larger distances than those for the 49-base oligomer. In order to predict the expected pulling distances, only two hairpin states were assumed: open and closed. [19–21] If a hairpin was closed at the time of the first encounter, the  $\beta$ -CD should stick at the first paired base in the stem. The distance, in bases, between predicted features in the force curve are shown under the sequences in Figures 4A and 4B, with the corresponding predicted contour lengths listed in Table 1. The corresponding distribution of measured contour lengths is given in Figures 4E and 4F. Peaks in these distributions are in good agreement with the predicted lengths, and the widths of the distributions are close to the expected 5.6 nm (Table 1 and solid lines in Figures 4E and F). Control pulls (lacking a CD altogether or taken with an unfunctionalized CD) showed no features beyond 62 nm (white bars).

### 2.3 Frequency of spontaneous hairpin opening

The free energies stabilizing these hairpins are quite small (Table 2) and the frequency of curves with only one feature corresponding to the second hairpin might be expected to give a measure of the spontaneous (unforced) opening rate of the first hairpin. It is open in 30% of the pulls for both the 49 base and 81 oligomer (it has the same stem sequence in both).  $\Delta G = -RT \ln ([open]/[closed])$  [21] yields  $\Delta G = 0.2$  kcal/mol, well below the 3.7 kcal/mol predicted by mFold. This underestimate is to be expected, because forced opening events for which the peak force is lower than the noise floor (ca. 20 pN) are not detected, and hence not counted in the denominator.

### 2.4 Magnitude of the opening force

The force required to open the hairpins by this method (up to 400 pN – Table 2) is remarkably large. Pulling apart the two strands that enter the double helical stem requires forces in the range of 10–15 pN, [21,22] consistent with the model of Cocco et al. [23] How could the same structure sustain a force some 40 times larger in the present geometry? The application of a force leads to unfolding as the work done on the folded molecule tilts the energy landscape towards the unfolded state. [21,22,24,25] For a single transition state that remains unchanged during the application of force, the distribution of opening forces is given by [24,25]

$$P(f) = \left[ \frac{1}{\tau_0} \exp\left(\frac{f}{f_B}\right) \right] \exp\left[ \frac{f_B}{\tau_0 r_f} \left( 1 - \exp\left(\frac{f}{f_B}\right) \right) \right] \quad (1)$$

where  $\tau_0$  is the mean time between thermal (unloaded) opening,  $r_f$  is the loading rate in N/s and  $f_B = k_B T / x_{TS}$  where  $x_{TS}$  is the distance from the equilibrium closed position to the position of the transition state for opening, measured along the reaction coordinate for unfolding. Solving Equation 1 for the modal value of the force ( $f^*$ ) yields

$$f^* = f_B \ln \left[ \frac{\tau_0 r_f}{f_B} \right] \quad (2)$$

The modal force is plotted as a function of loading rate for the three different hairpins in Figures 5A, C and E. The solid lines are fits to Equation 2 and these fits yield the values of  $\tau_0$  and  $x_{TS}$  listed in Table 2. As a check on the procedure, the parameters obtained by fitting Equation 2 were used to calculate the distribution of opening forces [Eq. 1] at a given loading rate for each of the hairpins. Calculated (solid lines) and measured force distributions are shown in Figures 5B, D and F. The thermal opening times at zero force – on the order of 10 to 100 ms – agree well with those reported by other methods. [6, 7, 22, 26] The key difference in this case lies in the much smaller distance to the transition state ( $x_{TS}$ ) measured here: 0.05 nm compared to the 5 to 26 nm measured when the force is applied via opposing strands. [21, 22] Thus the increased force required to open the hairpins by this method is a consequence of the much smaller strain required to destabilize the structure. More force is required to produce the destabilizing free energy because it acts over a shorter distance. The unfolding pathway is “brittle” compared to the pathway followed in experiments that pull on opposite ends of the double helical stem.

The kinetics of hairpin opening has been studied in a protein nanopore [6] yielding values for  $\tau_0$  which are with a factor of 3 to 10 times longer than the values we report here. It may be that we fail to sample the slowest events because of the relatively rapid force ramp used here. In the nanopore experiments, the quantity that is analogous to  $f_B$  is  $V_B$ , the bias that determines the voltage scale for electric-field driven opening.  $V_B$  is determined by the ratio of thermal energy to the charge acted on in the pore,  $k_B T / q$ , and thus does not yield information about the distance to a transition state. It is therefore not possible to compare the forces that act on the hairpin in the two experiments without a microscopic model of the nanopore.

### 3. Discussion

It is interesting to note that the spontaneous opening times do not correlate with the exponential of the stabilization free energy (Table 2) consistent with the results of experiments in which each DNA strand is pulled apart [23]. This discrepancy in both types of unfolding experiment demonstrates the importance of the transition state (as opposed to the equilibrium free energy difference) in these non-equilibrium opening measurements.

Some curves showed evidence of a third small feature at the fully stretched length of the oligomer (“End” in Table 1). Simulations [27] suggest that base-stacking plays a role in ‘feeding’ the polymer through the orifice, but once the CD is released from the phosphodiester backbone, it may form a complex with the terminal base, causing it to adhere to the end of the DNA. [28]

Polymers containing alternating blocks of purines and pyrimidines exhibited no composition-dependent signal above the noise level (Supporting Information). Therefore, this method does not appear to be capable of determining the DNA sequence with the current design, consistent with the predictions of a simulation. [29] It has, however, revealed unusually large unfolding forces and non-WLC stretching curves in some secondary structures that appear to cause enzymes to stall (Ashcroft et al. manuscript in preparation).

### 4. Conclusions

In conclusion, a novel nanomechanical molecular device with “tape-reading” capability has been demonstrated. AFM pulling of an encircling ring along a single-stranded DNA has been applied to secondary structure analysis. Disruption of hairpins by forced passage through the molecular ring occurs at much lower strains than those required to disrupt the secondary structure by pulling on the ends of the DNA. In consequence, a much larger force is required in order to provide the free energy necessary to destabilize the structure. The orifice used here is smaller than those encountered in biology and likely exaggerates this effect, but the data imply that the forces required to remove secondary structure depend strongly on the molecular detail of the unfolding pathway.

### 5. Experimental Section

#### 5.1 General

$\beta$ -cyclodextrin was a gift from Cargill Food and Pharma Specialties (Cedar Rapids, IA). (100 B-doped (50  $\Omega$ -cm) silicon wafers were products from Addison Engineering (San Jose, CA).. N-propyldimethylchlorosilane (*n*-propylsilane) and aminopropyldimethylethoxysilane (APDM) were purchased from Gelest, Inc. (Morrisville, PA), 3,3'-dithiobis(succinimidyl propionate) from Pierce Biotechnology, Inc. (Rockford, IL), N, N'-dicyclohexylcarbodiimide (DCC), N-hydroxysuccinimide (NHS) from Aldrich (Milwaukee, WI) along with all anhydrous solvents, and vinylsulfone-PEG-NHS (MW 3200) and maleimide-PEG-NHS (MW 5000) from Nektar Therapeutics (San Carlos, CA). All reagents were used as received. TLC plates were from EMD Chemical Inc (Gibbstown, NJ). Sephadex G-25 Quick Spin columns were from Roche Applied Science (Indianapolis, IN). Matrix assisted laser desorption ionization time-of-flight (MALDI-TOF) mass spectra were recorded on a VG ToFSpec spectrometer, Proteomics and Protein Chemistry Lab at Arizona State University. XPS spectra were recorded on XPS - Kratos XSAM800 with UHV ( $\sim 10^9$  Torr), LeRoy Eyring Center for Solid State Science. The ozone cleaner is a UV Clean #135500 (Boekel Inc.). Contact angles were measured using the EASYDROP Contact Angle Measuring System (Kruss) and ellipsometry was performed on an LSE Stokes Ellipsometer (Gaertner Scientific Corp.).

### 5.2 3, 3'-Dithiopropionic acid mono(N-mono-6-deoxy- $\beta$ -cyclodextrin)amide (S-CD)

Mono-6-deoxy-6-amino- $\beta$ -cyclodextrin ( $\beta$ -CD-NH<sub>2</sub>) was prepared following the literature [30] and characterized by MALDI mass spectrometry.  $\beta$ -CD-NH<sub>2</sub> (16 mg, 0.014 mmol) was dissolved in anhydrous DMF (10 mL) and added dropwise to a solution of 3,3'-dithiobis (succinimidyl propionate) (0.011 g, 0.028 mmol) in DMF (10 mL) with stirring under N<sub>2</sub>. [31] The reaction was monitored by TLC (isopropanol:ethyl acetate: ammonium hydroxide:water, 5:3:3:3), with the presence of the cyclodextrin product marked by treatment with 5% sulfuric acid in ethanol with heating. After completion of the reaction, the product mixture was rotary-evaporated down to ~2 mL of DMF. Acetone was added to the solution, the resulting precipitate gravity filtered, and washed with acetone. The precipitate was redissolved in the minimum amount of DMF, acetone was again added, and the precipitate collected. This process was repeated one more time. The final precipitate was dried *in vacuo* at 40°C overnight. The product was furnished as yellowish powder (73%). MALDI-TOF Mass (m/z): 1348 for [M + Na]<sup>+</sup> (calculated mass for (C<sub>48</sub>H<sub>79</sub>O<sub>37</sub>NS<sub>2</sub>): 1325). Further purification was carried out using preparative TLC (5:3:3:3 isopropanol:ethyl acetate:ammonium hydroxide:water, detected with H<sub>2</sub>SO<sub>4</sub> in ethanol) with *N*-hydroxysuccinimide byproduct used as a UV detectable marker and methanol used to extract the cyclodextrin (yield 49%). <sup>1</sup>H NMR (500MHz, D<sub>2</sub>O,  $\delta$ ): 5.24 (s, 1 H), 5.07 (s, 6 H), 3.94-3.61 (m, 42 H), 2.94 (t, 2 H), 2.60 (t, 2 H). We verified that this modified CD would form a rotaxane on a dodecyl-amine thread in solution (Figure s1 in the Supporting Information).

### 5.3 Silicon wafer pretreatment

Silicon wafers were cut into 1-cm square slabs and placed in the ozone cleaner for 10 minutes. The slabs were removed and immediately placed in piranha solution (3:1 sulfuric acid and hydrogen peroxide) for 3 minutes, and then rinsed with 18 M $\Omega$  water. Thickness of the oxidized layer: (3.3Å). Contact angle of the surface: 28°. *Caution: piranha solution is extremely corrosive and can explode on contact with organics!*

### 5.4 DNA conjugation on the CD-rotaxane surface

All oligonucleotides were deprotected with tris (2-carboxyethyl)phosphine hydrochloride (TCEP) (0.02% in PBS) for 15 minutes and run through a Sephadex G-25 size exclusion column before use, leaving a thiol linked to the DNA via a hexane linker. The thiolated DNA (0.75 nmol in 17  $\mu$ L of TCEP/PBS solution) was deposited on the CD-rotaxane surface (see Figure 2) and allowed to react for 2 hours. The synthesis of a surface bound CD-rotaxane was verified using FTIR (see Supporting Information, Figures s2 through s6). Sequences of all oligomers are given in the Supporting Information (Table s1).

### 5.5 Preparation of functionalized AFM probes

Ultrasharp CSC11/AIBS probes were placed in the ozone cleaner for 10 minutes, immediately dipped into fresh piranha solution for no more than 30 seconds (to prevent damage to the metallization), rinsed with water and put into a solution of APDM (200  $\mu$ L, 1.4  $\mu$ mol) in 95% ethanol (1 mL). After 5 minutes, the tips were rinsed with water, placed in a clean dessicator flushed with argon, and placed under vacuum (10 Torr) for 1 hour. The tips were removed from the vacuum and placed in solution of vinylsulfone -PEG-NHS (45 mg, 0.01 mmol) in PBS buffer (1 mL) pH 7 for 15 minutes. This produced tethered PEG molecules terminated in a vinylsulfone. The probes were then rinsed in water and used immediately. The maximum number of successful pulls with any one probe indicated that there were typically 15 to 45 functional groups near enough to the end of a probe to be used in the experiment.

## 5.6 Preparation of the system for pulling experiments

The final step in preparing the samples was addition of TCEP (0.02% in 50 mM phosphate buffer, pH 7) for 20 min to deprotect the thiols on the cyclodextrin. Surfaces were rinsed with PBS and force curves were obtained in PBS using the liquid cell of a Picoplus AFM (Molecular Imaging/Agilent).

## 5.7 Acquisition and analysis of force curves

The AFM was interfaced to a LabView control system via a custom modification of the AFM head electronics. The AFM approach was controlled with custom software using the Measurement Studio (National Instruments) in Visual Basic (Microsoft). Once all reagents were activated, the sample was placed immediately into the liquid cell of the microscope and covered in PBS buffer. A freshly-functionalized probe was inserted into the scanner and calibrated after each run using the thermal spectrum method. [32] The probe was lowered onto the surface using Measurement Studio until a deflection increase of  $\sim 100$  pN was detected, held for 6–8 s to allow the linkers to react, and then retracted while force-distance curves were recorded. Pulls showing significant deflection at a distance greater than 50 nm from the surface were flagged for further analysis. Typically, 80 retractions from the surface were required to locate one successful pull because the substrate surface had been sparsely functionalized in order to present only an individual linker for reaction with the tip for any given pull. Each probe lasted  $\sim 800$  to 1000 pulls before all the active tethers were depleted (through the collection of  $\sim 15$  to 45 curves that were indicative of successful attachment to the S-CD). Each sample survived through 3 probe replacements to give a total of 3000 curves per run. The end of the experiment was signaled by the appearance of spurious features at distances greater than the sum of the linker and DNA lengths (indicative of contamination). 2000 data points per second were collected for each force-distance curve at pulling rates that varied from 30 nm/s to 600 nm/s. Rupture of the rotaxane system occurred close to the surface at higher pulling speeds, limiting the maximum loading rates (see Supporting Information).

Displacement data were corrected for the tip deflection, and all plots shown here reflect the true probe-sample distance.

## Supplementary Material

Refer to Web version on PubMed Central for supplementary material.

## References

1. Jeruzalmi D, O'Donnell M, Kuriyan J. *Curr Opin Struct Biol* 2002;12:217–224. [PubMed: 11959500]
2. Bustamante C, Smith SB, Liphardt J, Smith D. *Current Opinion in Structural Biology* 2000;10:279–285. [PubMed: 10851197]
3. Bustamante C, Bryant Z, Smith SB. *Nature* 2003;421:423–427. [PubMed: 12540915]
4. Keyser UF, Koelman BN, van Dorp S, Krapf D, Smeets RMM, Lemay SG, Dekker NH, Dekker C. *Nature Physics* 2006;2:473–477.
5. Sanchez-Quesada J, Saghatelian A, Cheley S, Bayley H, Ghadiri MR, Reza M. *Angew Chem Int Ed* 2004;43:3063–3067.
6. Mathe J, Visram H, Viasnoff V, Rabin Y, Meller A. *Biophysical Journal* 2004;87:3205–3212. [PubMed: 15347593]
7. Vercoutere WA, Winters-Hilt S, DeGuzman VS, Deamer D, Ridino SE, Rodgers JT, Olsen HE, Marziali A, Akeson M. *Nucleic Acids Research* 2003;31:1311–1318. [PubMed: 12582251]
8. Sauer-Budge AF, Nyamwanda JA, Lubensky DK, Branton D. *Phys Rev Lett* 2003;93:238101–238105. [PubMed: 12857290]
9. Bension, RM. U S Patent. 7163658. Jan 17. 2007

10. Sauvage, J-P.; Dietrich-Buchecker, C. *Molecular Catenanes, Rotaxanes and Knots: A Journey Through the World of Molecular Topology*. Wiley; New York: 1999.
11. Gibson, HW.; Mahan, EJ. *Cyclic Polymers*. 2. Semlyen, JA., editor. Springer; Berlin: 2000. p. 415-560.
12. Dodziuk, H. Wiley-VCH; New York: 2006.
13. Smith SB, Cui Y, Bustamante C. *Science* 1996;271:795–799. [PubMed: 8628994]
14. Timothy, V Ratto; Langry, Kevin C.; Rudd, Robert E.; Balhorn, Rodney L.; Allen, Michael J.; McElfresh, MW. *Biophysical Journal* 2004;86:2430–2437. [PubMed: 15041680]
15. Oesterhelt F, Rief M, Gaub HE. *New Journal of Physics* 1999;1:6.1–6.11.
16. Bustamante C, Marko JF, Siggia ED, Smith S. *Science* 1994;265:1599–1600. [PubMed: 8079175]
17. Grandbois G, Beyer M, Rief M, Clausen-Schaumann H, Gaub HE. *Science* 1999;283:1727–1703. [PubMed: 10073936]
18. Carrion-Vazquez M, Oberhauser AF, Fowler SB, Marszalek PE, Broedel SE, Clarke J, Fernandez JM. *Proc Natl Acad Sci U S A* 1999;96:3694–3699. [PubMed: 10097099]
19. Cuesta-Lopez S, Peyrard M, Graham DJ. *The European Physical Journal E* 2005;16:235–246.
20. Muth J, Williams PM, Williams SJ, Brown MD, Wallace DC, Karger BL. *Electrophoresis* 1996;17:1875–1883. [PubMed: 9034769]
21. Liphardt J, Onoa B, Smith SB, Tinoco I Jr, Bustamante C. *Science (Washington, DC, United States)* 2001;292:733–737.
22. Greenleaf WJ, Woodside MT, Abbondanzieri EA, Block SM. *Phys Rev Lett* 2005;95.
23. Cocco S, Monasson R, Marko JF. *PNAS* 2001;98:8608–8613. [PubMed: 11447279]
24. Evans E, Ritchie K. *Biophys J* 1997;72:1541–1555. [PubMed: 9083660]
25. Evans E. *Annual Review of Biophysics and Biomolecular Structure* 2001;30:105–128.
26. Dornberger U, Leijon M, Fritzsche H. *J Biol Chem* 1999;274:6957–6962. [PubMed: 10066749]
27. Flores S, Echols N, Milburn D, Hespeneheide B, Keating K, Lu J, Wells S, Yu EZ, Thorpe MF, Gerstein M. *Nucleic Acid Research* 2006;34:D296–D301.
28. Spies MA, Schowen RL. *J Am Chem Soc* 2002;124:14049–14053. [PubMed: 12440903]
29. Qamar S, Williams PM, Lindsay SM. *Biophysical Journal*. 2007submitted
30. Petter RC, Salek JS, Sikorski CT, Kumaravel G, Lin FT. *J Am Chem Soc* 1990;112:3860–3868.
31. Henke C, Steinem C, Janshoff A, Steffan G, Luftmann H, Sieber M, Galla HJ. *Analytical Chemistry* 1996;68:3158–3165.
32. Hutter JL, Bechhoefer J. *Review of Scientific Instruments* 1993;64:1868–1873.

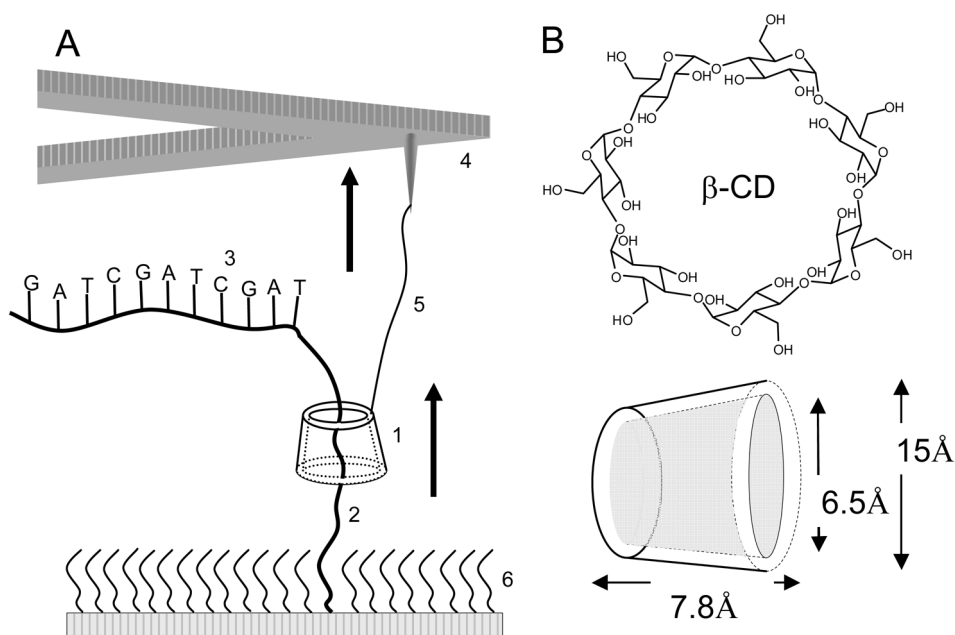


**Figure 1.** (A) AFM-rotaxane for sequential reading of DNA secondary structure. The  $\beta$ -cyclodextrin ring (1), previously self-threaded onto a surface-tethered molecule, is pulled up over a 28 nm long PEG molecule (2) and onto a DNA oligomer (3) attached to the PEG at its 5' end. An AFM probe (not to scale) (4) has successfully “fished” for the  $\beta$ -CD with a functionalized PEG linker (5). The molecular threads that capture the  $\beta$ -CD are embedded in a ‘non-stick’ matrix (6) to minimize spurious adhesion and contamination. (B) Structure and dimensions of  $\beta$ -cyclodextrin.

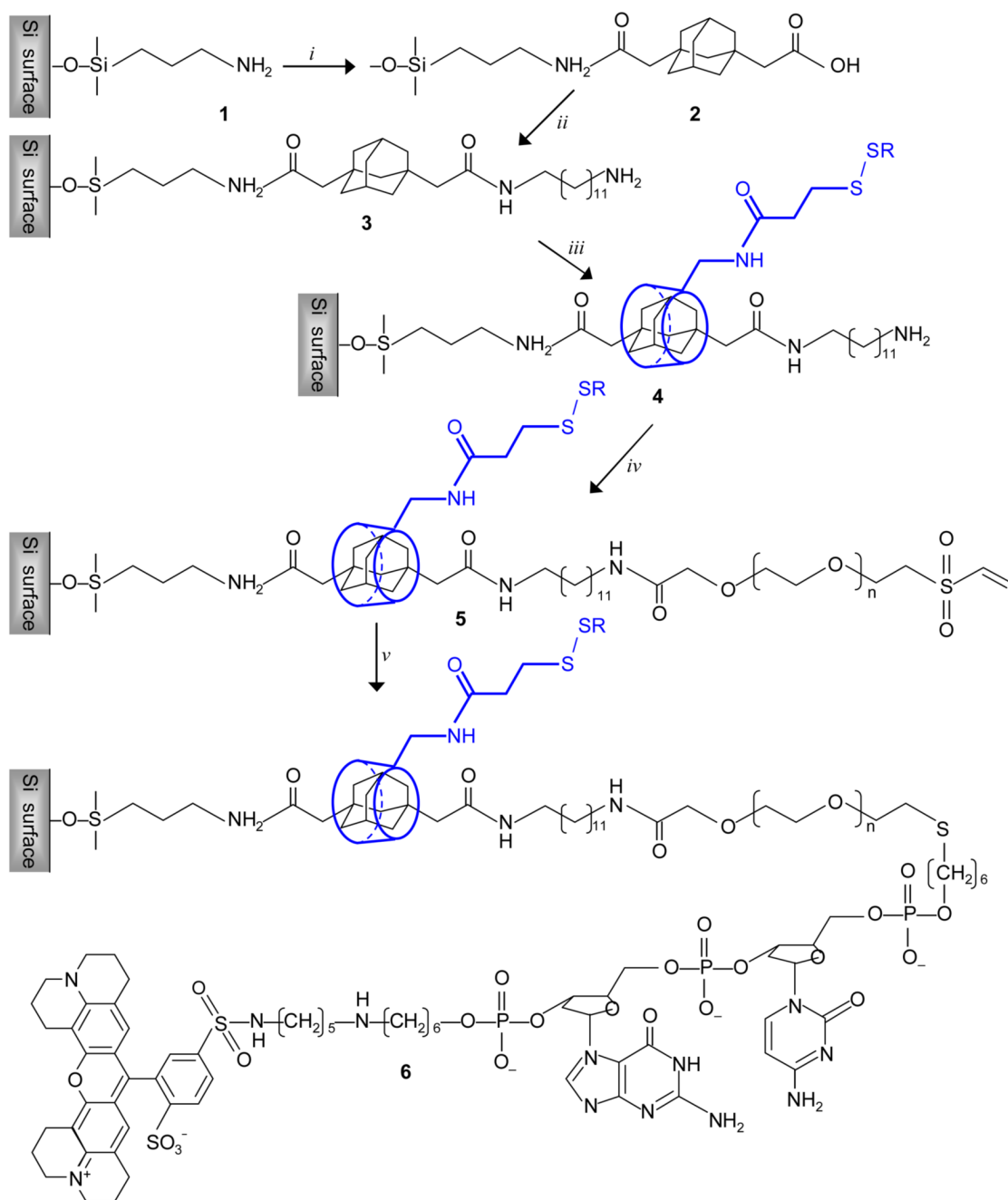


**Figure 2.**

Assembly of DNA conjugated rotaxanes on the aminopropylsilylated silicon surface. *Reagents and conditions:* (i) 1,3-adamantane diacetic acid, dicyclohexylcarbodiimide (DCC), *N*-hydroxysuccinimide 50 °C, 15 min; (ii) *N*-hydroxysuccinimide, DCC, 10 min, then 1,12-diaminododecane; (iii) 3, 3'-Dithiopropionic acid mono(*N*-mono-6-deoxy- $\beta$ -cyclodextrin) amide, 20 min; (iv) vinyl sulfone-PEG-NHS, 30 min; (v) thiol functionalized oligonucleotide.

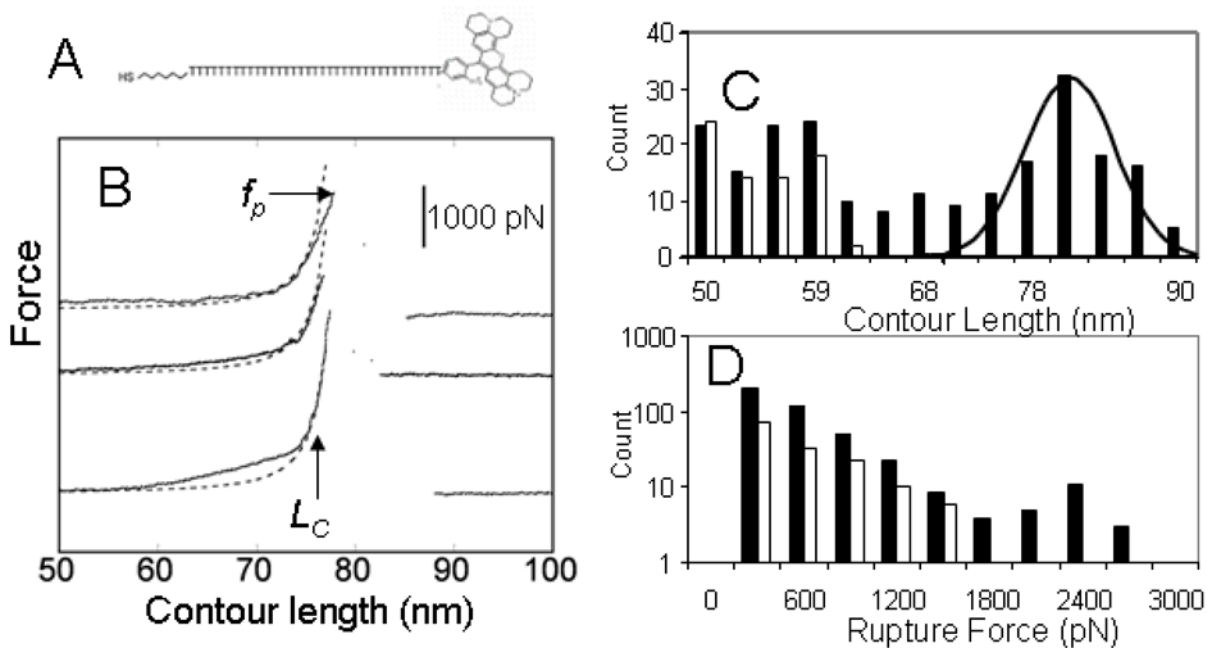


**Figure 3.**

Passage of a covalently-stoppered DNA lacking secondary structure. (A) The T<sub>35</sub> oligomer is thiolated at its 5' and stoppered at its 3' end by a large dye molecule. (B) Examples of force-distance curves (with arbitrary vertical displacements) that show features out beyond the stretched tether length of 62 nm (all distances are corrected for tip displacement). The polymer contour length,  $L_C$ , is derived from fits of the worm-like chain model (dashed lines). (C) Distribution of measured values of  $L_C$ . Black bars are data for the full construct using all curves that yielded data beyond 62 nm. White bars show data for controls lacking a CD or taken with a CD that lacked functionalization. The solid line is a Gaussian centered at 80 nm with a HWHH of 5.6 nm. (D) Distribution of peak forces,  $f_p$ . White bars are controls.

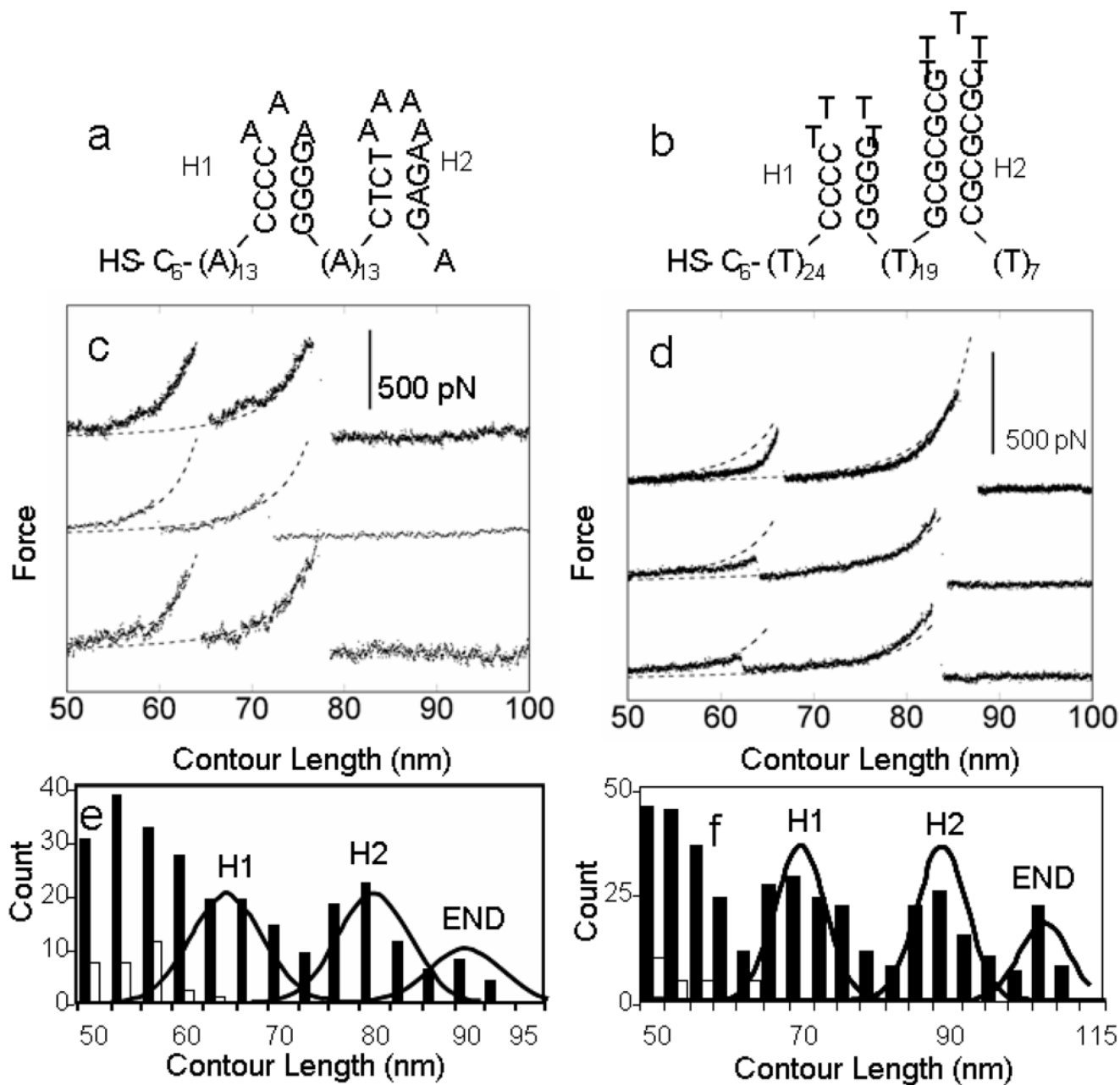


**Figure 4.**

Passage of two DNA molecules (A and B) each containing two hairpins. Examples of force curves for the 49 base oligomer (A) are given in C and for the 81 base oligomer (B) in (D). Dotted lines are fits to the WLC model. The distribution of pulling lengths,  $L_C$ , for the 49 base oligomer (E) and the 81 base oligomer (F). Solid lines are Gaussians of HWHH 5.6 nm centered at the positions shown in Table 1.

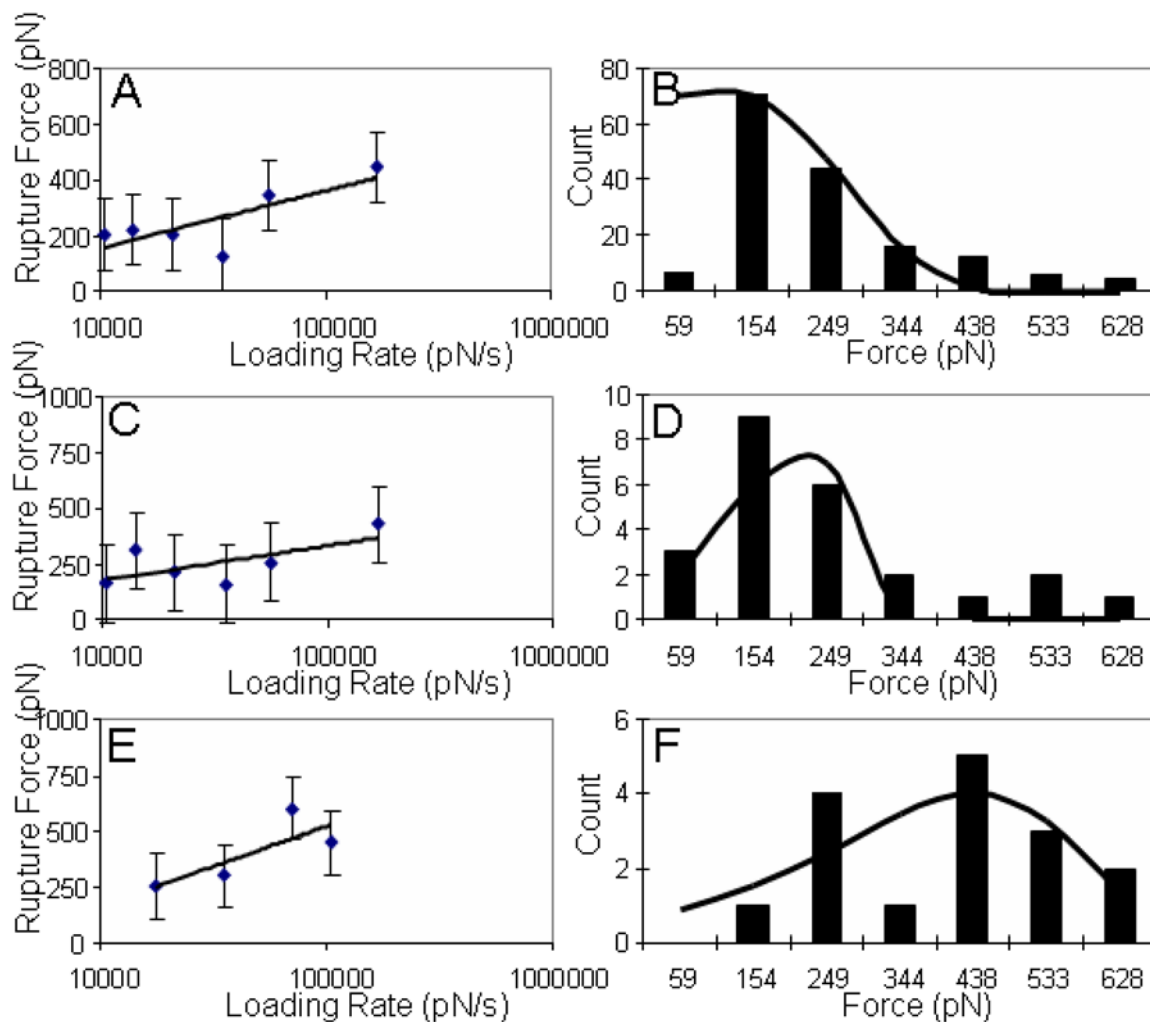


**Figure 5.** Kinetic analysis of hairpin opening: The left panels plot the modal force (error bars are  $\pm 1$  sd) as a function of the logarithm of the loading rate for (A) the first hairpins in both oligomers (data were identical and are aggregated here) (C) the second hairpin in the 49 base oligomer and (E) the second hairpin in the 81 base oligomer. The corresponding distribution of measured forces are plotted in the right panels at loading rates of 10.5 nN/s (B) 21 nN/s (D) and 105 nN/s (F) The solid lines are calculated with equation 1 using the parameters shown in Table 2.

**Table 1**

Predicted ( $d$ ) and measured ( $L_C$ ) distances to peaks in the force-distance curves. Measured values are systematically a few nm lower than the predicted values probably owing to the tip geometry (radius ca. 5 nm, so that most active tethers are suspended some nm above the point of contact).  $L_C$  was obtained from fits of the WLC model. Corresponding values of the effective persistence length  $L_p$  are listed as the mean values and a range (because the s.d. usually exceeds the mean). The number of curves analyzed is  $n$  (with the subset that yielded reliable values for  $L_p$  in parenthesis)

Feature	$d$ (nm)	$L_C$ (nm)	$L_p$ (nm)	$N$
End, T <sub>35</sub> test sample	83±5.6	80±6	0.2 (0.05 to 1.0)	108(10)
1 <sup>st</sup> hairpin, 49 base oligomer	70±5.6	66±5	0.4 (0.05 to 1.0)	58(36)
2 <sup>nd</sup> hairpin, 49 base oligomer	85±5.6	81±5.6	0.3 (0.05 to 0.8)	66(27)
End, 49 base oligomer	91±5.6	89±5	0.3 (0.05 to 0.9)	15(7)
1 <sup>st</sup> hairpin, 81 base oligomer	78±5.6	73±6	0.4 (0.05 to 0.8)	125(20)
2 <sup>nd</sup> hairpin, 81 base oligomer	96±5.6	94±6	0.3 (0.05 to 1.0)	81(20)
End, 81 base oligomer	110±5.6	103±8	0.3 (0.05 to 1.0)	37(4)

**Table 2**

Average rupture forces for the various secondary structures (data for the hairpins with identical stems have been combined).  $x_{rs}$  and  $\tau_{open}$  were derived from fits to equation 2. Stabilization free energies ( $\Delta G$ ) are predicted by mFold

Feature	$\langle f_p \rangle$ (pN)	$x_{rs}$ (nm)	$\tau_{open}$ (ms)	$\Delta G_{calc}$ (kcal/mole)
1 <sup>st</sup> hairpin, both oligomers	376	0.05±0.01	53±56	-5.95
2 <sup>nd</sup> hairpin, 49 base oligomer	248	0.06±0.01	100±37	-2.94
2 <sup>nd</sup> hairpin, 81 base oligomer	371	0.03±0.01	43±26	-12.19